Effective field theory for proton halo nuclei

Emil Ryberg,[1] Christian Forssén,[1] H.-W. Hammer,[2,3,4] and Lucas Platter[1,5,*]

[1]*Department of Fundamental Physics, Chalmers University of Technology, SE-412 96 Göteborg, Sweden*

[2]*Helmholtz-Institut für Strahlen- und Kernphysik, Universität Bonn, 53115, Bonn, Germany*

[3]*Institut für Kernphysik, Technische Universität Darmstadt, 64289 Darmstadt, Germany*

[4]*ExtreMe Matter Institute (EMMI), GSI Helmholtzzentrum für Schwerionenforschung, 64291 Darmstadt, Germany*

[5]*Physics Division, Argonne National Laboratory, Argonne, Illinois 60439, USA*

(Received 1 November 2013; revised manuscript received 10 December 2013; published 29 January 2014)

We use halo effective field theory to analyze the universal features of proton halo nuclei bound due to a large S-wave scattering length. Our work provides a fully field-theoretical treatment of bound halo nuclei in the presence of a repulsive Coulomb interaction. With a Lagrangian built from effective core and valence-proton fields, we derive a leading-order expression for the charge form factor. Within the same framework we also calculate the radiative proton capture cross section. We present general results at leading order that can be applied to any one-proton halo system bound in a relative S wave. We illustrate the method by studying the excited $1/2^+$ state of fluorine 17, for which we give results for the charge radius and the astrophysical S factor.

DOI: 10.1103/PhysRevC.89.014325 PACS number(s): 11.10.Ef, 21.10.Gv, 21.30.Fe, 25.40.Lw

I. INTRODUCTION

Exotic isotopes along the neutron and proton drip lines are important for our understanding of the formation of elements and they constitute tests of our understanding of nuclear structure. The proton- and neutron-rich regimes in the chart of nuclei are therefore the focus of existing and forthcoming experimental facilities around the world [1]. The emergence of new degrees of freedom is one important feature of these systems, exemplified, e.g., by the discovery of several nuclear halo states along the drip lines [2–4]. Halo states in nuclei are characterized by a tightly bound core with weakly attached valence nucleon(s). Universal structures of such states can be considered a consequence of quantum tunneling, where tightly bound clusters of nucleons behave coherently at low energies and the dynamics is dominated by relative motion at distances beyond the region of the short-range interaction. In the absence of the Coulomb interaction, it is known that halo nuclei bound due to a large positive S-wave scattering length will show universal features [5,6]. In the case of proton halo nuclei, however, the Coulomb interaction introduces an additional momentum scale k_C, which is proportional to the charge of the core and the reduced mass of the halo system. The low-energy properties of proton halos strongly depend on k_C.

Halo effective field theory (EFT) is the ideal tool to analyze the features of halo states with a minimal set of assumptions. It describes these systems using their effective degrees of freedom, i.e., core and valence nucleons, and interactions that are dictated by low-energy constants [7,8]. For S-wave proton halo systems there will be a single unknown coupling constant at leading order (LO), and this parameter can be determined from the experimental scattering length, or the one-proton separation energy. Obviously, halo EFT is not intended to compete with *ab initio* calculations that, if applicable, would aim to predict low-energy observables from computations starting with a microscopic description of the many-body system. Instead, halo EFT is complementary to such approaches as it provides a low-energy description of these systems in terms of effective degrees of freedom. This reduces the complexity of the problem significantly. By construction, it can also aid to elucidate the relationship between different low-energy observables.

Furthermore, halo EFT is built on fields for clusters, which makes it related to phenomenological few-body cluster models [3]. The latter have often been used successfully for confrontation with data for specific processes involving halo nuclei. A relevant example in the current context is the study of proton radiative capture into low-lying states states of ^{17}F [9]. A general discussion of electromagnetic reactions of proton halos in a cluster approach was given in Ref. [10]. The emphasis of an EFT, however, is the systematic expansion of the most general interactions and, as a consequence, the ability to estimate errors and to improve predictions order by order. The possibility to determine higher-order parameters in the EFT is crucial to be competitive with traditional approaches in terms of precision. A promising strategy is to combine halo EFT with microscopic *ab initio* approaches. Certain quantities that are computed in the latter can be used directly to fix EFT parameters. In particular, low-energy scattering observables and asymptotic normalization coefficients can be computed microscopically [11–13], and there are a couple of recent examples of how such results are employed as input for EFT calculations [14,15]. The structure and reactions of one- and two-neutron halos have been studied in halo EFT over the past years (see, e.g., Refs. [16–22]). However, concerning charged systems, only unbound states such as $\alpha\alpha$ [23] and αp [24] have been treated in halo EFT.

In this work, we apply halo EFT for the first time to one-proton halo nuclei. We use a fully field-theoretical approach based on the irreducible self-energy. A distinct advantage of this approach for bound-state calculations is that the calculation of the self-energy at the bound-state pole allows a

*lplatter@phy.anl.gov

direct determination of the wave function renormalization. We restrict ourselves to LO calculations of systems that are bound due to a large S-wave scattering length between the core and the proton. Observables are calculated with a minimal set of assumptions, and we are able to derive universal formulas that describe (to a certain accuracy) any S-wave, one-proton halo system as function of the charge of the core, the mass ratio, and the proton separation energy. However, for applications where the expansion parameter is not very small, high-precision calculations will require the inclusion of higher orders in the EFT expansion.

The manuscript is organized as follows: In Sec. II, we introduce the halo EFT and discuss how Coulomb interactions are treated within this framework. In the following section, we present our results and calculate, in particular, the charge form factor and charge radius at LO. Furthermore, we derive expressions for the radiative capture cross section. We apply our general formulas to the excited $1/2^+$ state of ^{17}F and compare our numerical results with existing data for this system. The expansion parameter of our EFT is estimated based on the separation of scales for typical energies involved. We conclude with an outlook and a discussion on the importance of higher-order corrections.

II. THEORY

In halo EFT, the core and the valence nucleons are taken as the degrees of freedom. For a one-proton halo system, with a spin-zero core, the Lagrangian is given by

$$\mathcal{L} = \sum_{k=0,1} \psi_k^\dagger \left(i\mathrm{D}_0 + \frac{\mathbf{D}^2}{2m_k} \right) \psi_k - C_0 \psi_0^\dagger \psi_1^\dagger \psi_1 \psi_0 + \cdots . \quad (1)$$

Here ψ_0 denotes the proton field with mass m_0, ψ_1 denotes the core field with mass m_1, C_0 denotes the LO coupling constant, and the dots denote derivative operators that facilitate the calculation of higher-order corrections. The covariant derivative is defined as $\mathrm{D}_\mu := \partial_\mu + ie\hat{\mathrm{Q}}A_\mu$, where $\hat{\mathrm{Q}}$ is the charge operator. The resulting one-particle propagator is given by

$$iS_k(p_0,\mathbf{p}) = i\left[p_0 - \frac{\mathbf{p}^2}{2m_k} + i\varepsilon \right]^{-1}. \quad (2)$$

For convenience, we also define the proton-core two-particle propagator

$$iS_{\mathrm{tot}}(p_0,\mathbf{p}) = i\left[p_0 - \frac{\mathbf{p}^2}{2m_{\mathrm{R}}} + i\varepsilon \right]^{-1}, \quad (3)$$

where m_{R} denotes the reduced mass of the proton-core system. We include the Coulomb interaction through the full Coulomb Green's function

$$\langle \mathbf{k}|G_{\mathrm{C}}(E)|\mathbf{p}\rangle = -S_{\mathrm{tot}}(E,\mathbf{k})\chi(\mathbf{k},\mathbf{p};E)S_{\mathrm{tot}}(E,\mathbf{p}), \quad (4)$$

where χ is the Coulomb four-point function defined recursively in Fig. 1. To distinguish coordinate-space from momentum-space states, we denote the former with round brackets, i.e., $(\mathbf{r}|$. In coordinate space, the Coulomb Green's function can be expressed via its spectral representation

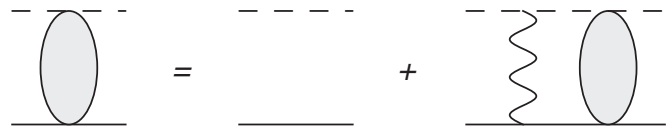

FIG. 1. The integral equation for the four-point function $\chi(\mathbf{k}_1,\mathbf{k}_2)$. The dashed line denotes a core propagator, the solid line denotes a proton propagator, and the wavy line denotes the exchange of a Coulomb photon.

$$(\mathbf{r}|G_{\mathrm{C}}(E)|\mathbf{r}') = \int \frac{d^3p}{(2\pi)^3} \frac{\psi_{\mathbf{p}}(\mathbf{r})\psi_{\mathbf{p}}^*(\mathbf{r}')}{E - \mathbf{p}^2/(2m_{\mathrm{R}}) + i\varepsilon}, \quad (5)$$

where we define the Coulomb wave function through its partial wave expansion

$$\psi_{\mathbf{p}}(\mathbf{r}) = \sum_{l=0}^{\infty} (2l+1) i^l \exp(i\sigma_l) \frac{F_l(\eta,\rho)}{\rho} P_l(\hat{\mathbf{p}}\cdot\hat{\mathbf{r}}). \quad (6)$$

Here we have defined $\rho = pr$ and $\eta = k_{\mathrm{C}}/p$, with the Coulomb momentum $k_{\mathrm{C}} = Z_{\mathrm{c}}\alpha m_{\mathrm{R}}$, and also the pure Coulomb phase shift $\sigma_l = \arg\Gamma(l+1+i\eta)$. For the Coulomb functions F_l and G_l, we use the conventions of Ref. [25]. The regular Coulomb function F_l can be expressed in terms of the Whittaker M function according to

$$F_l(\eta,\rho) = A_l(\eta) M_{i\eta,l+1/2}(2i\rho), \quad (7)$$

with the A_l defined as

$$A_l(\eta) = \frac{|\Gamma(l+1+i\eta)| \exp[-\pi\eta/2 - i(l+1)\pi/2]}{2(2l+1)!}. \quad (8)$$

We also need the irregular Coulomb wave function, G_l, which is given by

$$G_l(\eta,\rho) = iF_l(\eta,\rho) + B_l(\eta) W_{i\eta,l+1/2}(2i\rho), \quad (9)$$

where W is the Whittaker W function and the coefficient B_l is defined as

$$B_l(\eta) = \frac{\exp(\pi\eta/2 + il\pi/2)}{\arg\Gamma(l+1+i\eta)}. \quad (10)$$

To obtain the fully dressed two-particle propagator, that includes strong and Coulomb interactions, we calculate the irreducible self-energy shown in Fig. 2:

$$\begin{aligned} i\Sigma(E) &= -i \int \frac{d^3k_1 d^3k_2}{(2\pi)^6} S_{\mathrm{tot}}(E,\mathbf{k}_1)\chi(\mathbf{k}_1,\mathbf{k}_2)S_{\mathrm{tot}}(E,\mathbf{k}_2) \\ &= i(0|G_{\mathrm{C}}(E)|0). \end{aligned} \quad (11)$$

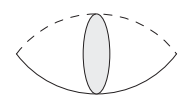

FIG. 2. The irreducible self energy at LO. The solid (dashed) line denotes the proton (core) propagator. The shaded blob denotes the Coulomb Green's function.

The expression above is known and is given by

$$(0|G_{\rm C}(E)|0) = -2m_R \int \frac{d^3q}{(2\pi)^3} \frac{\psi_{\mathbf{q}}(0)\psi^*_{\mathbf{q}}(0)}{q^2 - 2m_R E - i\varepsilon}. \quad (12)$$

This integral was solved in Ref. [26], using dimensional regularization in the power divergence subtraction (PDS) scheme, as

$$\Sigma(E) = -\frac{k_{\rm C} m_{\rm R}}{\pi} H(\eta) + \Sigma^{\rm div}, \quad (13)$$

with a divergent part $\Sigma^{\rm div}$

$$\Sigma^{\rm div} = \frac{k_{\rm C} m_{\rm R}}{\pi}\left[\frac{1}{3-d} + \log\left(\frac{\sqrt{\pi}\mu}{2k_{\rm C}}\right) + 1 - \frac{3C_{\rm E}}{2}\right] - \frac{m_{\rm R}\mu}{2\pi}, \quad (14)$$

where d is the space dimension, $C_{\rm E}$ is the Euler constant, and μ is the PDS regulator. The function H is defined as

$$H(\eta) = \psi(i\eta) + \frac{1}{2i\eta} - \log(i\eta), \quad (15)$$

with ψ being the polygamma function. Note that the divergent part in Eq. (14) is energy independent. This will become important later when the derivative of Σ, with respect to the energy, will be required.

The coupling constant C_0 can be determined by matching to a two-body observable, such as the Coulomb corrected proton-core scattering length [26]:

$$\frac{1}{a_{\rm C}} = \frac{2\pi}{m_{\rm R}}\left(\frac{1}{C_0} - \Sigma^{\rm div}\right). \quad (16)$$

Since we stay at LO, however, an explicit expression for C_0 will not be required for the calculation of electromagnetic observables in the next section.

III. RESULTS

A. Charge form factor

In our calculation of the charge form factor, we follow the derivation of the deuteron form factor presented in Ref. [27]. The form factor is obtained by calculating the matrix element

$$\langle \mathbf{p}'|J^0_{\rm EM}|\mathbf{p}\rangle = e(Z_c+1)F_{\rm C}(\mathbf{Q}^2), \quad (17)$$

for momentum transfer $\mathbf{Q} = \mathbf{p}' - \mathbf{p}$ in the Breit frame, where no energy is transferred by the photon. It was shown in Ref. [27] that this matrix element can be expressed as [28]

$$\langle \mathbf{p}'|J^0_{\rm EM}|\mathbf{p}\rangle = \frac{\Gamma^0(\mathbf{Q})}{\Sigma'(-B)}, \quad (18)$$

where Γ^0 denotes the irreducible three-point function shown in Fig. 3, and $\Sigma'(-B)$ is the derivative of the self energy with respect to the total energy evaluated at the energy $E = -B$, where B is the proton separation energy or core-proton binding energy.

With the proton-core mass ratio $f = m_0/m_1$, the three-point function Γ^0 is given by

$$\Gamma^0(\mathbf{Q}) = -eZ_{\rm c}\int d^3r \exp(if\mathbf{Q}\cdot\mathbf{r})|(0|G_{\rm C}(-B)|\mathbf{r})|^2 + [(f \to 1-f),(Z_{\rm c}\to 1)], \quad (19)$$

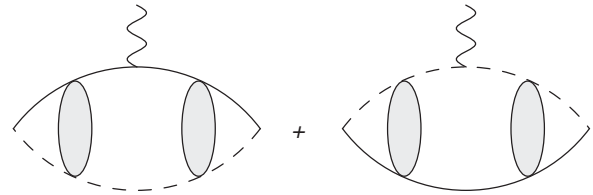

FIG. 3. The irreducible three-point function Γ^0.

and the derivative of the self-energy can be written as

$$\Sigma'(-B) = -\int \frac{d^3q}{(2\pi)^3} \frac{\psi_{\mathbf{q}}(0)\psi^*_{\mathbf{q}}(0)}{[B + \mathbf{q}^2/(2m_R)]^2}. \quad (20)$$

Evaluating Γ^0 at zero momentum transfer, by using Eq. (5) and orthonormality of the wave functions, and comparing it with Eq. (20) shows that the charge form factor is properly normalized to one in this limit.

We find that Eq. (19) can be simplified by writing the Coulomb Green's function for negative energy using the Whittaker W function. This is achieved by demanding proper asymptotics and using that only the S-wave part can contribute to propagation to zero separation, that is,

$$\begin{aligned}(0|G_{\rm C}(-B)|\mathbf{r}) &= \lim_{\rho'\to 0}\left(-i\frac{m_{\rm R}\gamma_0}{2\pi}\frac{F_0(\eta,\rho')[iF_0(\eta,\rho)+G_0(\eta,\rho)]}{\rho'\rho}\right)\\ &= i\frac{m_{\rm R}\Gamma(1+k_{\rm C}/\gamma_0)}{2\pi}\frac{W_{-k_{\rm C}/\gamma_0,1/2}(2\gamma_0 r)}{r}, \end{aligned} \quad (21)$$

where we have introduced the binding momentum $\gamma_0 = \sqrt{2m_{\rm R}B}$. The resulting integral is then

$$\Gamma^0(\mathbf{Q}) = -\frac{em_{\rm R}^2\Gamma(1+k_{\rm C}/\gamma_0)^2}{\pi}\int dr\, W_{-k_{\rm C}/\gamma_0,1/2}(2\gamma_0 r)^2 \times\{Z_{\rm c} j_0(fQr) + j_0[(1-f)Qr]\}, \quad (22)$$

where j_l are the spherical Bessel functions. Once the parameters of the proton halo system are fixed, the equation

$$F_{\rm C}(\mathbf{Q}^2) = \frac{\Gamma^0(\mathbf{Q})}{e(Z_c+1)\Sigma'(-B)} \quad (23)$$

is used to calculate the charge form factor and the corresponding charge radius numerically. We have calculated these quantities for the excited $1/2^+$ state of ^{17}F, which has a proton separation energy of $B = 104.94(35)$ keV [29]. Note that the proton separation energy is the only nontrivial experimental input at LO.

The charge form factor is related to the charge radius via the expansion

$$F_{\rm C}(\mathbf{Q}^2) = 1 - \frac{\langle r^2_{\rm C}\rangle_{\rm rel}}{6}\mathbf{Q}^2 + \cdots, \quad (24)$$

and we find for the charge radius squared

$$\langle r^2_{\rm C}\rangle_{\rm rel} = (0.59\ \ {\rm fm})^2. \quad (25)$$

Since the proton and core are treated as structureless fields in halo EFT, this quantity corresponds to the charge radius

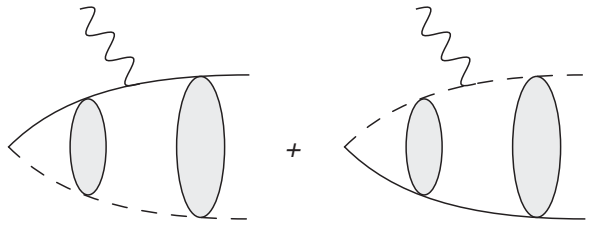

FIG. 4. The radiative proton capture diagrams.

difference according to

$$\langle r_C^2\rangle_{^{17}F^*} = \frac{Z_c}{Z_c+1}\langle r_C^2\rangle_{^{16}O} + \frac{1}{Z_c+1}\langle r_C^2\rangle_p + \langle r_C^2\rangle_{rel}, \quad (26)$$

where $\langle r_C^2\rangle_X$ is the charge radius squared corresponding to the particle $X = {}^{17}F^*$, ${}^{16}O$, p. Analog to the deuteron case, the charge radii of proton and ${}^{16}O$ enter at higher orders in the calculation via counterterms.

The error of the EFT can be estimated by comparing the momentum scale $k_{lo} \sim \gamma_0$ of the halo with the breakdown scale k_{hi} of the EFT. The latter is given by the closest interfering state. For the ${}^{17}F$ halo system the breakdown scale is given by the bound state, $E_0 = 495.33(10)$ keV below the $1/2^+$ state [29]. Thus, the expected LO error is $\gamma_0/\sqrt{2m_R E_0} \approx 50\%$ for the halo state in ${}^{17}F^*$, which is comparable to the LO error of a pionless EFT calculation for the two-nucleon system. Higher orders in the EFT are required, however, for high-precision calculations. Performing a next-to-leading-order (NLO) calculation is beyond the scope of this paper but will be the topic of future work.

B. Radiative capture

Our approach can easily be applied to low-energy radiative capture. The differential cross section for this reaction is

$$\frac{d\sigma}{d\Omega} = \frac{m_R\omega}{8\pi^2 p}\sum_{i=1}^{2}\left|\epsilon_i\cdot\frac{\mathcal{A}}{\sqrt{\Sigma'(-B)}}\right|^2, \quad (27)$$

where $\mathcal{A}$ is the vector amplitude for the sum of the diagrams shown in Fig. 4, where a proton is captured by a core while a real photon is emitted. The relative momentum of the proton-core system is $\mathbf{p}$ and the four-momentum of the photon is $(\omega,\omega\hat{z})$, with associated polarization vectors $\epsilon_1 = \hat{x}$ and $\epsilon_2 = \hat{y}$. The factor $1/\sqrt{\Sigma'(-B)}$ is the wave function renormalization, or LSZ reduction factor.

The vector amplitude $\mathcal{A}$ can be expressed as the integral

$$\mathcal{A} = \frac{eZ_c f}{m_R}\int d^3r[(0|G_C(-B)|\mathbf{r})\exp(-if\omega r\cos\theta) \times(\nabla\psi_{\mathbf{p}}(\mathbf{r}))] + [(f\to 1-f),(Z_c\to 1)], \quad (28)$$

where the ∇ has emerged from the Feynman rule of the vector photon coupling and acts on the Coulomb wave function due to a partial integration. By evaluating the angular integrals and multiplying with the polarization vector, the integral is

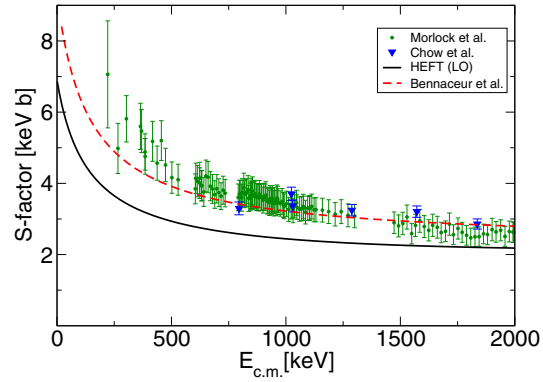

FIG. 5. (Color online) The LO halo EFT result for the astrophysical S factor for ${}^{16}O(p,\gamma){}^{17}F^*(1/2^+)$ is presented by the solid black line. The theoretical result is compared with the data by Chow *et al.* [30] and Morlock *et al.* [31,32] shown by blue (gray) triangles and green (gray) dots, respectively. The calculation by Bennaceur *et al.* [33] is shown by the dashed curve.

simplified to

$$\sum_{i=1}^{2}|\epsilon_i\cdot\mathcal{A}|^2 = \Bigg|-i\sin\theta(\cos\phi+\sin\phi)\frac{4\pi eZ_c f\exp(i\sigma_1)}{m_R p} \times\int dr(0|G_C(-B)|\mathbf{r})j_0(f\omega r) \times\frac{\partial}{\partial r}[rF_1(k_C/p,pr)] +[(f\to 1-f),(Z_c\to 1)]\Bigg|^2, \quad (29)$$

where the angles θ and ϕ will be integrated over to give the total cross section. For a given physical system, we can solve the integral in Eq. (29) numerically using Eq. (21) for the Coulomb Green's function.

Radiative capture into low-lying states of ${}^{17}F$ has been measured by Rolfs *et al.* [9], Chow *et al.* [30], and Morlock *et al.* [31,32]. In Fig. 5 we show the astrophysical S factor, defined as

$$S(E) = E\exp(2\pi\eta)\sigma_{tot}. \quad (30)$$

The figure shows the halo EFT results of our LO calculation compared to experimental data for capture into the $1/2^+$ excited state and a phenomenological calculation using the shell model embedded in the continuum. At threshold, we find that $S(0) \approx 7$ keVb. Our LO results are slightly low but consistent with the experimental data, within the expected 50% error. To improve the precision in higher-order calculations, the corresponding low-energy constants must be determined. Ideally this can be done from other experiments. In the case of the S factor for ${}^{16}O(p,\gamma){}^{17}F^*(1/2^+)$, there will be contribution from the effective range in elastic ${}^{16}O$-p scattering at NLO. At higher orders the shape parameter and electromagnetic low-energy constants will contribute as well. The effective-range parameters in elastic ${}^{16}O$-p scattering can in principle be determined by fitting an appropriate EFT expression to a phase-shift analysis such as in Ref. [34]. The EFT might

have to include the ^{17}F ground state explicitly in order to be applicable at energies of order 2 MeV. One can also imagine that new experimental data should become available from, e.g., ion storage rings [35]. The use of stripped ion beams in combination with windowless gas-jet targets could offer an opportunity to extract high-quality, low-energy scattering data. Alternatively, the effective range could be determined from an experimental extraction of the asymptotic normalization constant of the ^{17}F$^*(1/2^+)$ excited state. (See, e.g., Ref. [36] for an extraction from transfer reactions.) Electromagnetic two-body currents, which will contribute at higher orders, may be determined from the inverse reaction and from *ab initio* input. A detailed analysis of higher order contributions is left for a future publication. However, we anticipate that the NLO correction will increase the radiative capture cross section through the appearance of a finite effective range at this order. It can also be noted that the results agree qualitatively with the predictions obtained in the shell model embedded in the continuum [33]. While the shell-model approach is clearly more sophisticated, our approach starts from a very different outset. Observables are calculated with a minimal set of assumptions and the LO result represents a prediction based on universality.

IV. CONCLUSIONS

In this work, we have shown that Coulomb effects can be included in halo EFT and that thereby static and dynamical observables of proton halo nuclei become accessible. We have calculated the charge radius and the radiative proton capture cross section of S-wave proton halo nuclei at LO in halo EFT. Our results can be applied to any one-proton halo system whose interaction is dominated by S waves. In particular, the excited $1/2^+$ state in ^{17}F is known to have a large S-wave component. We have calculated the charge radius for this system. While this observable is not yet experimentally accessible, this result provides a prediction for *ab initio* calculations using modern nucleon-nucleon interactions.

In addition, we have compared our results for radiative capture into the excited $1/2^+$ state of ^{17}F with experimental data and found good agreement within the expected error. Furthermore, we found that halo EFT gives the same qualitative behavior for this observable as previous calculations that have employed phenomenological models.

For a quantitative description of the experimental data, higher order corrections are required. In a future publication, we will address how these corrections are included within halo EFT in the presence of Coulomb interactions. The size of these contributions will strongly be affected by the relative size of the effective range and the Coulomb momentum k_C, which provides an additional scale in systems with Coulomb interactions. Our calculation is also a first step towards a calculation of properties of ^{8}B within halo EFT. This system requires the inclusion of two low-energy constants at LO since it interacts dominantly in the P wave [7].

Finally, our approach might prove useful for heavier systems whose static observables can be calculated using *ab initio* approaches but for which continuum properties are not accessible within the same framework due to the computational complexity. In this scenario, *ab initio* predictions of, e.g., the one-proton separation energy could be used to fix the halo EFT parameters, which in turn could be used to predict continuum observables such as the radiative capture cross section. In the case of neutron halos, such an approach was recently carried out to predict novel features in the Calcium isotope chain using halo EFT [14]. More recently, asymptotic normalization coefficients from variational Monte Carlo have been used to fix the LO parameters of an EFT calculation of radiative ^{7}Li neutron capture [15]. Continued work along these lines is expected as higher order EFT calculations become available and demand the determination of additional low-energy parameters.

ACKNOWLEDGMENTS

We thank H. Esbensen and S. König for helpful discussions and P. Mohr and K. Bennaceur for supplying relevant data. This work was supported by the Swedish Research Council (No. 2010-4078), the European Research Council under the European Community's Seventh Framework Program (FP7/2007-2013) / ERC Grant No. 240603, the Office of Nuclear Physics, U.S. Department of Energy under Contract No. DE-AC02-06CH11357, the DFG and the NSFC through the Sino-German CRC 110, the BMBF under Contract No. 05P12PDFTE, and the Helmholtz Association under Contract No. HA216/EMMI.

[1] M. Thoennessen and B. Sherrill, Nature (London) **473**, 25 (2011).
[2] B. Jonson, Phys. Rep. **389**, 1 (2004).
[3] A. S. Jensen, K. Riisager, and D. V. Fedorov, Rev. Mod. Phys. **76**, 215 (2004).
[4] K. Riisager, Phys. Scr. **T152**, 014001 (2013).
[5] E. Braaten and H.-W. Hammer, Phys. Rep. **428**, 259 (2006).
[6] H.-W. Hammer and L. Platter, Philos. Trans. R. Soc., A **369**, 2679 (2011).
[7] C. Bertulani, H.-W. Hammer, and U. van Kolck, Nucl. Phys. A **712**, 37 (2002).
[8] P. F. Bedaque, H.-W. Hammer, and U. van Kolck, Phys. Lett. B **569**, 159 (2003).
[9] C. Rolfs, Nucl. Phys. A **217**, 29 (1973).
[10] S. Typel and G. Baur, Nucl. Phys. A **759**, 247 (2005).
[11] S. Quaglioni and P. Navrátil, Phys. Rev. Lett. **101**, 092501 (2008).
[12] K. M. Nollett and R. B. Wiringa, Phys. Rev. C **83**, 041001 (2011).
[13] G. Hagen and N. Michel, Phys. Rev. C **86**, 021602 (2012).
[14] G. Hagen, P. Hagen, H.-W. Hammer, and L. Platter, Phys. Rev. Lett. **111**, 132501 (2013).
[15] X. Zhang, K. M. Nollett, and D. R. Phillips, arXiv:1311.6822.
[16] D. L. Canham and H.-W. Hammer, Eur. Phys. J. A **37**, 367 (2008).
[17] H.-W. Hammer and D. R. Phillips, Nucl. Phys. A **865**, 17 (2011).
[18] G. Rupak and R. Higa, Phys. Rev. Lett. **106**, 222501 (2011).

[19] G. Rupak, L. Fernando, and A. Vaghani, Phys. Rev. C **86**, 044608 (2012).
[20] J. Rotureau and U. van Kolck, Few Body Syst. **54**, 725 (2013).
[21] P. Hagen, H.-W. Hammer, and L. Platter, Eur. Phys. J. A **49**, 118 (2013).
[22] B. Acharya, C. Ji, and D. R. Phillips, Phys. Lett. B **723**, 196 (2013).
[23] R. Higa, H.-W. Hammer, and U. van Kolck, Nucl. Phys. A **809**, 171 (2008).
[24] R. Higa, EPJ Web Conf. **3**, 06001 (2010).
[25] S. Koenig, D. Lee, and H.-W. Hammer, J. Phys. G: Nucl. Part. Phys. **40**, 045106 (2013).
[26] X. Kong and F. Ravndal, Phys. Lett. B **450**, 320 (1999).
[27] D. B. Kaplan, M. J. Savage, and M. B. Wise, Phys. Rev. C **59**, 617 (1999).
[28] The reason for the additional factor of $-i$ in our Eq. (18) compared to Eq. (A10) of Ref. [27] is that we have an extra $-i$ in our definition of the irreducible self-energy.
[29] D. Tilley, H. Weller, and C. Cheves, Nucl. Phys. A **564**, 1 (1993).
[30] H. C. Chow, G. M. Griffiths, and T. H. Hall, Can. J. Phys. **53**, 1672 (1975).
[31] R. Morlock, R. Kunz, A. Mayer, M. Jaeger, A. Müller, J. W. Hammer, P. Mohr, H. Oberhummer, G. Staudt, and V. Kölle, Phys. Rev. Lett. **79**, 3837 (1997).
[32] C. Iliadis, C. Angulo, P. Descouvemont, M. Lugaro, and P. Mohr, Phys. Rev. C **77**, 045802 (2008).
[33] K. Bennaceur, F. Nowacki, J. Okołowicz, and M. Płoszajczak, Nucl. Phys. A **671**, 203 (2000).
[34] R. A. Blue and W. Haeberli, Phys. Rev. **137**, B284 (1965).
[35] Y. Litvinov, S. Bishop, K. Blaum, F. Bosch, C. Brandau, L. Chen, I. Dillmann, P. Egelhof, H. Geissel, R. Grisenti *et al.*, Nucl. Instr. Meth. Phys. Res. B **317**, 603 (2013).
[36] C. A. Gagliardi, R. E. Tribble, A. Azhari, H. L. Clark, Y.-W. Lui, A. M. Mukhamedzhanov, A. Sattarov, L. Trache, V. Burjan, J. Cejpek *et al.*, Phys. Rev. C **59**, 1149 (1999).